JACS
JOURNAL OF THE AMERICAN CHEMICAL SOCIETY
Communication
pubs.acs.org/JACS

Piezofluorochromic Metal–Organic Framework: A Microscissor Lift

Qiang Zhang,[†] Jie Su,*[,‡] Dawei Feng,[†] Zhangwen Wei,[†] Xiaodong Zou,[‡] and Hong-Cai Zhou*[,†]

[†]Department of Chemistry, Texas A&M University, College Station, Texas 77843, United States

[‡]Berzelii Centre EXSELENT on Porous Materials and Inorganic and Structural Chemistry, Department of Materials and Environmental Chemistry, Stockholm University, Stockholm 106 91, Sweden

Supporting Information

ABSTRACT: We have successfully constructed a metal–organic framework, denoted as PCN-128W, starting from chromophoric linker and zirconium salt. PCN-128W exhibits interesting piezofluorochromic behavior, the color reversibly changes from white to yellow and so does the emission maximum from 470 to 538 nm. The stepwise fluorescence change was monitored by fluorospectroscopy which demonstrated gradual shift of the emission maximum when sequential compression was exerted. In order to gain deep insights into the piezofluorochromic mechanism, both the white and yellow phases are structurally characterized.

Piezofluorochromic[1] materials attract increasing interest in both fundamental studies and practical applications owing to their unique photophysical properties that change in response to external stimuli.[2] This class of materials has been widely used in luminescence switches, mechanosensors, data storage, and security papers.[3] A number of piezofluorochromic organic, organometallic, and a few 1D or 2D coordination polymers have been reported in the past decade.[4] However, low reversibility and loss of fluorescence or crystallinity occur frequently, when chemical or physical treatments were applied.[4a,5] Therefore, discovery of new stimuli-responsive materials with high reversibility, tunable luminescence, and maintenance of crystallinity throughout the transformation is highly desirable.

Metal–organic frameworks (MOFs) are an intriguing class of inorganic–organic hybrid crystalline materials with high porosity and internal surface areas.[6] The tunability through either predesigned linkers or postsynthetic modifications makes MOFs great candidates for a variety of applications.[7] Fluorescent MOFs have attracted great interests for their unique photophysical properties and applications.[8] Recently, tetraphenylethylene (TPE)-based linkers have been introduced into MOFs.[9] However, these MOFs are constructed from soft metals,[10] which make them unsuitable for sensing in aqueous solutions. Thus, MOFs with high chemical stability are desired for sensing for a wide range of substrates under various conditions.

Herein, we report a new stable Zr-MOF that is prepared from H_4ETTC[11] (4′,4‴,4⁗,4⁗′-(ethene-1,1,2,2-tetrayl)tetrakis(([1,1′-biphenyl]-4-carboxylic acid))) and eight-connected Zr_6 clusters, denoted as PCN-128W (PCN stands for porous coordination network, W stands for white). PCN-128W contains one of the largest known 1D open channels among MOFs with the same topology, with a diameter of the hexagonal channel up to 4.3 nm. A unique piezofluorochromic behavior of PCN-128W was observed, which is mainly due to conformation change of the linker upon stimulation. The photoluminescence (PL) variation of PCN-128W, which corresponds to the transformation of the ETTC linker, was spectroscopically monitored. The MOF maintains its crystallinity throughout, and both the color and the emission changes are fully reversible.

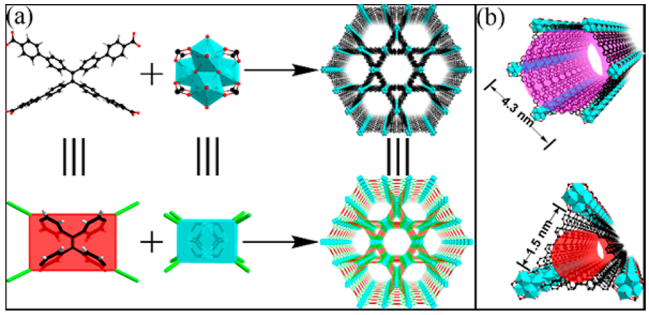

Figure 1. (a) Construction of PCN-128W from the ETTC linker and Zr_6 cluster. (b) Two types of 1D channels in PCN-128W, the hexagonal channel (purple pillar) and the triangular channel (red pillar).

It has been revealed that the conformation of TPE-based linkers is different from their free forms, when they are incorporated into MOF backbones.[9,11,12] However, under most circumstances, the MOF matrix restricts the linker frame from further distortion, thus limiting the flexibility of the TPE core. Having this concern, we designed a MOF that contains the ETTC linker and eight-connected Zr_6 clusters. The simulated structure is very similar to that of PCN-222 except ETTC is used instead of TCPP (tetrakis(4-carboxyphenyl)-porphyrin) as shown in Figure 1a.[13] The feature of this designed MOF is that the symmetry of the framework would allow the ETTC linker to alter its conformation, which presumably will impact the luminescence of the MOF. Bearing this in mind, we sought to synthesize PCN-128W starting from H_4ETTC and $ZrCl_4$. It is well-known that the architecture of MOFs is very sensitive to the synthetic conditions. Starting from the same ligand and metal salt, different phases can be obtained. This phenomenon has been extensively demonstrated in the porphyrin-zirconium MOF family.[14]

White crystalline powder of PCN-128W was obtained under solvothermal conditions with trifluoroacetic acid (TFAA) as the competing reagent. As we expected, PCN-128W was found to change its color from white to yellow when compressed with a glass slide or treated with 6.0 M HCl solution as described

Received: May 5, 2015
Published: July 27, 2015

DOI: 10.1021/jacs.5b04695
J. Am. Chem. Soc. 2015, 137, 10064–10067

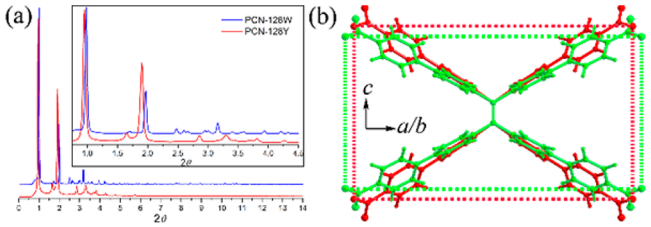

Figure 2. (a) Synchrotron-based PXRD patterns of PCN-128W (blue) and PCN-128Y (red). (b) Comparison of ETTC linkers in PCN-128W (red) and PCN-128Y (green).

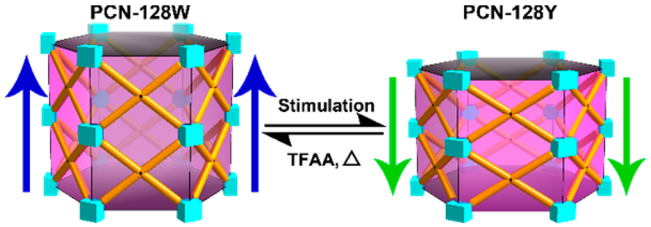

Figure 3. Simplified schematic diagram illustrating the reversible motion of the microscissor lift in ascent (left) and descent (right) modes represent PCN-128W and PCN-128Y, respectively.

previously.[15] The yellow powder PCN-128Y (Y stands for yellow) shows similar but distinct PXRD pattern compared to PCN-128W. High-resolution synchrotron-based PXRD measurements were also carried out for both PCN-128W and PCN-128Y to further evaluate the differences. In contrast with PCN-128W, the diffraction peaks of PCN-128Y in the low angle region (<2°) are shifted to lower angles and the peaks in region 2.5−5.0° are obviously different, Figure 2a.

In order to confirm the successful synthesis of the targeted PCN-128W structure, rotation electron diffraction (RED)[16] was applied to collect the 3D electron diffraction data of PCN-128W (Figures S5, S6), from which the unit cell parameters and space group were determined. An initial structural model was obtained from the RED data by direct methods. To obtain further insights into the structural relationship between PCN-128W and PCN-128Y, Rietveld refinement was carried out against the synchrotron PXRD data of each sample starting from the initial structural model (SI), which converged to a R_{wp} value of 0.0526 for PCN-128W and 0.0583 for PCN-128Y. It turns out that the structures of PCN-128W and PCN-128Y are very similar, both consisting of Zr_6 clusters linked by rectangular ETTC planar ligands (Figure 1a). In PCN-128W, the coordination sites between Zr_6 clusters were refined as trifluoroacetate (TFA) groups (Figure S8). In contrast, all the equatorial sites in PCN-128Y are occupied by terminal OH/H_2O groups. The framework contains two types of 1D open channels, the hexagonal channel with a diameter of 4.3 nm for PCN-128W and 4.4 nm for PCN-128Y, which are among the largest reported channels in MOFs that adopt the same topology, and the triangular channel with a diameter of 1.5 nm, as shown in Figure 1b.

Although PCN-128W and PCN-128Y belong to the same space group (*P6/mmm*) and the same topology (**csq-a**), the unit cell parameters, however, are slightly different. The size and shape of the rectangle formed between four oxygen atoms in the ETTC linker are different, with 18.9 × 11.7 Å for PCN-128W (Figure 2b (red)) and 19.7 × 10.0 Å for PCN-128Y (Figure 2b (green)). As discussed above, the unique topology of PCN-128W allows ETTC to change its conformation like a pair of scissors. The framework can be viewed as a microscissor lift that is constructed by folding supports, in a criss-cross "X" pattern (ETTC linkers), linked through pivot points (Zr_6 SBUs). PCN-128W can be considered as the ascent mode shown in Figure 3, both sides of the scissors will be able to "close" upon compression, and the entire framework shrinks along the *c* axis according to the pantograph mechanism to yield PCN-128Y, which can be regarded as the descent mode. Remarkably, the whole process is reversible. The upward motion of the microlift can be achieved when PCN-128Y is treated with TFAA in DMF at elevated temperature (SI). This is also in a good agreement with the structure of PCN-128W in which two TFA groups were attached oppositely to the adjacent Zr_6 clusters. The presence of TFA groups in PCN-128W but not

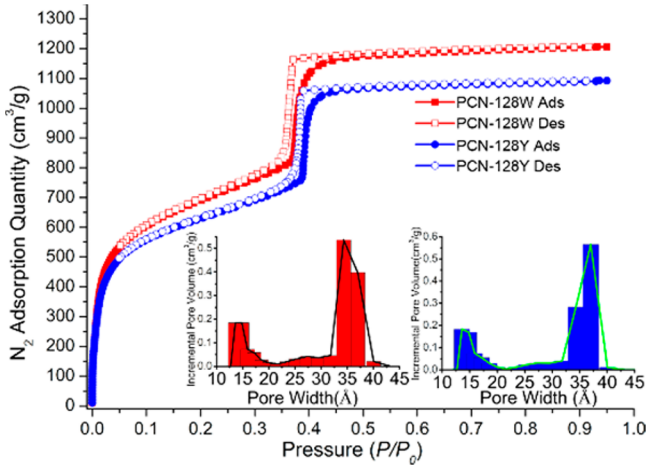

Figure 4. N_2 adsorption−desorption isotherms and pore size distributions (insets) of PCN-128W (red squares) and PCN-128Y (blue circles). Ads stands for adsorption (solid filled squares or circles) and Des stands for desorption (no filled squares or circles). Insets are pore size distributions for PCN-128W (left) and PCN-128Y (right).

in PCN-128Y is also supported by the X-ray energy dispersive spectroscopy (EDS) analysis (SI, Section S8).

Knowing the unit cell parameters and structural relationship between PCN-128W and PCN-128Y, we anticipate to see difference in gas adsorption−desorption isotherms. As discussed above, the ETTC linker diminishes along the *c* axis, and beyond doubt, it simultaneously stretches in the *ab* plane, which will further amplify the diameter of the 1D channel. The nitrogen adsorption−desorption isotherms of PCN-128W and PCN-128Y were then investigated to further support our assumption. As shown in Figure 4, type IV isotherms were observed, with a steep increase at the P/P_0 value of 0.378 for PCN-128W and 0.393 for PCN-128Y, suggesting the mesoporosity nature and indicating larger pores are present in PCN-128Y. Nitrogen uptake of 1207 $cm^3 \cdot g^{-1}$ (STP), Brunauer−Emmett−Teller (BET) surface area of 2532 $m^2 \cdot g^{-1}$, and Langmuir surface area of 5273 $m^2 \cdot g^{-1}$ were calculated from the adsorption measurements for PCN-128W and nitrogen uptake of 1094 $cm^3 \cdot g^{-1}$ (STP), BET surface area of 2349 $m^2 \cdot g^{-1}$, and Langmuir surface area of 4774 $m^2 \cdot g^{-1}$ for PCN-128Y. Density functional theory (DFT) simulations indicate that there are two types of pores in each form, with sizes of 1.5 and 3.5 nm for PCN-128W and 1.5 and 3.8 nm for PCN-128Y (Figure 4 insets), assigned to triangular microchannels and hexagonal mesochannels, respectively. While the change of the micro-channel is not obvious, the meso-channel has clearly been enlarged from 3.5 to 3.8 nm along with the phase transformation, which further supports the structure refinement results in which PCN-128Y contains larger channels.

DOI: 10.1021/jacs.5b04695
J. Am. Chem. Soc. 2015, 137, 10064−10067

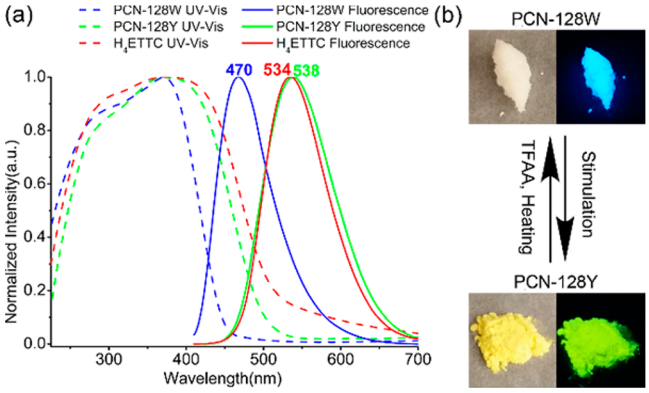

Figure 5. (a) Diffuse reflectance spectra of PCN-128W (dashed blue line), PCN-128Y (dashed green line), and H4ETTC (dashed red line) and fluorescent spectra of PCN-128W (solid blue line), PCN-128Y (solid green line), and H_4ETTC (solid red line) at room temperature. (b) The color of PCN-128W and PCN-128Y under room light (left) and under UV light (right).

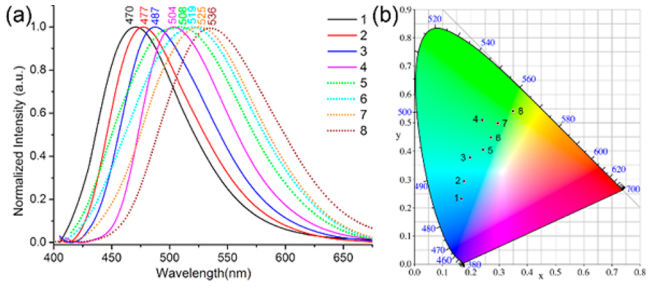

Figure 6. Emission changes when PCN-128W is transferred to PCN-128Y. (a) Change of the emission maximum when compression was applied: 1, PCN-128W (black solid line); 2, first compression (red solid line); 3, second compression (blue solid line); 4, third compression (pink solid line); 5, after treatment of DMF (green dotted line); 6, first compression after the treatment (cyan dotted line); 7, second compression after the treatment (orange dotted line); and 8, third compression after the treatment (brown dotted line). (b) The CIE color space chromaticity diagram showing changes of the emission color gradually from blue to green-yellow. The numbers 1−8 correspond to the ones in (a).

Apart from the framework structure and pore size variation, the conformation of ETTC linker will predominantly impact the photophysical properties of the MOF. Keeping this in mind, the solid-state absorption measurements of PCN-128W, PCN-128Y, and H_4ETTC were conducted using diffuse reflectance spectroscopy. H_4ETTC exhibits a broad absorption ranging from 225 to 500 nm, whereas PCN-128W exhibits sharper absorption from 225 to 450 nm, which is clearly blue-shifted. Interestingly, the absorption of PCN-128Y is very similar to that of H_4ETTC. Both PCN-128Y and H_4ETTC are yellow owing to their absorption of blue light, but PCN-128W is white because it only absorbs UV light, see Figure 5a dashed lines.

TPE is a conventional fluorophore which is well-known for its aggregation-induced emission character.[12] Therefore, the solid-state PL of PCN-128W and PCN-128Y as well as H_4ETTC were studied. While the freshly prepared PCN-128W emits bright blue light measured at 470 nm, surprisingly, the activated PCN-128Y emits green light observed at 538 nm which is almost 70 nm red-shifted and is similar to that of H_4ETTC (534 nm), as shown in Figure 5a. PCN-128W is a white powder under room light and emits blue light under 365 nm irradiation. However, PCN-128Y is yellow under room light and green under 365 nm UV light as shown in Figure 5b. More significantly, as mentioned previously, not only the color but also the PL are completely reversible. The reversible transformation of the structure and color as well as luminescence indicates that PCN-128W is a piezofluorochromic MOF.

As stated above, the coordination sites on the equatorial plane between Zr_6 clusters are occupied by TFA groups in PCN-128W. These coordinated TFA groups, together with solvent molecules, add strains to ETTC linkers and lock them in an "open" conformation, which increases their HOMO−LUMO energy gap and gives rise to high energy emission.[11] When PCN-128W is treated with strong acid, the coordinated trifluoroacetate groups can be removed and replaced by OH/H_2O groups, which are much smaller and will mostly remove the hindrance between Zr_6 clusters. ETTC linkers can then be fully relaxed to generate PCN-128Y. In the case of dry sample, there are no solvent molecules to stabilize the framework, thus the ETTC linkers relax in a slow fashion at room temperature in air. When grinding or compression was applied, the dry PCN-128W changed color immediately to yellow, indicating the phase transformation has taken place. It is important to note that PCN-128W undergoes negligible changes even after months if it was soaked in common organic solvents like DMF and acetone. However, the dry sample changes gradually from white to yellow in air for 1 week. For PCN-128W, the inner pressure is altered by attaching and eliminating the TFA groups between Zr_6 clusters, which causes the microlift to move upward and downward, respectively. Recently a supramolecular-jack-like MOF has been reported, in which a guest dependent thermal expansion behavior was discovered.[17]

Even if the transformation from PCN-128W to PCN-128Y is a slow process, the similarity in X-ray diffraction patterns makes it difficult to identify the transformation intermediates. On the other hand, fluorescence is very sensitive to linker conformation, thus it is possible to monitor the phase change via fluorospectroscopy. While as-synthesized PCN-128W emitted at 470 nm in Figure 6a, by placing the white powder on a PXRD sample holder and compressing it with a glass slide, the emission maximum was shifted to 477 nm. When the sample was compressed for the second time, the emission peak was further shifted to 487 nm. The peak was found at 504 nm after the third time compression, and a light-yellow powder was obtained. Surprisingly, no further shift was observed even after compressing the light-yellow powder sample for hours. This is probably due to the coordinated TFA groups, which restricted the Zr_6 clusters to move closer, thus stopping the ETTC linkers from further deformation. If this would be the case, based on the foregoing statement, PCN-128Y, which emits at 538 nm, could be realized after removing those TFA groups.

To support our hypothesis, the sample, which emitted at 504 nm, was soaked in DMF for 12 h at room temperature and washed thoroughly with DMF, acetone and dried at 65 °C. The emission maximum was found at 508 nm after the treatment. Upon compression, the peak migrated to 519 nm and 525 nm, respectively. Finally the emission of PCN-128Y at 536 nm was detected after the third time compression of the DMF treated sample. The CIE color space chromaticity diagram in Figure 6b shows the gradual migration of emission color from blue to green-yellow step by step. Spots 1−4 represent the emission color before DMF wash, and spots 5−8 represent emission color after the DMF treatment. It is clear that the solid and dotted lines in Figure 6a are two different stages, with and without TFA groups, since

DOI: 10.1021/jacs.5b04695
J. Am. Chem. Soc. 2015, 137, 10064−10067

the emission colors of those two groups belong to different phases as illustrated in Figure 6b.

The aforementioned results demonstrated a piezofluorochromic MOF, PCN-128W, which is constructed from TPE-based linkers and Zr_6 clusters. The luminescence of PCN-128W is bathochromically shifted from 470 to 538 nm to form PCN-128Y by change of the exterior (physical) or interior (chemical) pressures. The process is fully reversible by treating PCN-128Y with TFAA in DMF at elevated temperature. The study of the transformation mechanism indicates that PCN-128W can be considered as a microscissor lift. This work illustrates a very rare example of reversible 3D piezofluorochromic MOF. Besides, PCN-128W is highly stable in water and acidic or basic conditions (SI). MOFs with tunable fluorescence are promising candidates for applications in photocatalysis and sensing. Work along these directions is currently in progress.

■ ASSOCIATED CONTENT

Supporting Information

The Supporting Information is available free of charge on the ACS Publications website at DOI: 10.1021/jacs.5b04695.

CCDC-1062875 (PCN-128W) and CCDC-1062876 (PCN-128Y) contains the supplementary crystallographic data. Experimental procedures, structure refinement details and material characterizations (PDF)

Characterization data (CIF)

Characterization data (CIF)

■ AUTHOR INFORMATION

Corresponding Authors

*jie.su@mmk.su.se

*zhou@chem.tamu.edu

Notes

The authors declare no competing financial interest.

■ ACKNOWLEDGMENTS

The photophysical studies of this research was supported by the Center for Gas Separations Relevant to Clean Energy Technologies, an Energy Frontier Research Center funded by the U.S. Department of Energy, Office of Science, Office of Basic Energy Sciences under award no. DE-SC0001015. The structural analysis by RED and PXRD was supported by the Swedish Research Council (VR), the Swedish Governmental Agency for Innovation Systems (VINNOVA), Röntgen-Ångström Cluster and the Knut & Alice Wallenberg Foundation through a grant for purchasing the TEM and the project grant 3DEM-NATUR. The authors also acknowledge the financial supports of ARPA-e funded by the U.S. Department of Energy under award no. DE-AR0000249 and Welch Foundation under award no. A-1725. Use of the Advanced Photon Source, an Office of Science User Facility operated for the U.S. Department of Energy (DOE) Office of Science by Argonne National Laboratory, was supported by the U.S. DOE under award no. DE-AC02-06CH11357. The authors also like to thank Dr. Amanda Young from TAMU Materials Characterization Facility for the help and valuable discussion.

■ REFERENCES

(1) Bouas-Laurent, H.; Dürr, H. *Pure Appl. Chem.* **2001**, *73*, 639.

(2) (a) Caruso, M. M.; Davis, D. A.; Shen, Q.; Odom, S. A.; Sottos, N. R.; White, S. R.; Moore, J. S. *Chem. Rev.* **2009**, *109*, 5755. (b) Jeong, C. K.; Kim, I.; Park, K.-I.; Oh, M. H.; Paik, H.; Hwang, G.-T.; No, K.; Nam, Y. S.; Lee, K. J. *ACS Nano* **2013**, *7*, 11016.

(3) (a) Irie, M.; Fukaminato, T.; Sasaki, T.; Tamai, N.; Kawai, T. *Nature* **2002**, *420*, 759. (b) Sagara, Y.; Kato, T. *Nat. Chem.* **2009**, *1*, 605. (c) Yan, D.; Lu, J.; Ma, J.; Qin, S.; Wei, M.; Evans, D. G.; Duan, X. *Angew. Chem., Int. Ed.* **2011**, *50*, 7037. (d) Kwon, M. S.; Gierschner, J.; Yoon, S.-J.; Park, S. Y. *Adv. Mater.* **2012**, *24*, 5487. (e) Lim, S.-J.; An, B.-K.; Jung, S. D.; Chung, M.-A.; Park, S. Y. *Angew. Chem., Int. Ed.* **2004**, *43*, 6346. (f) Hirata, S.; Watanabe, T. *Adv. Mater.* **2006**, *18*, 2725. (g) Kishimura, A.; Yamashita, T.; Yamaguchi, K.; Aida, T. *Nat. Mater.* **2005**, *4*, 546.

(4) (a) Chi, Z.; Zhang, X.; Xu, B.; Zhou, X.; Ma, C.; Zhang, Y.; Liu, S.; Xu, J. *Chem. Soc. Rev.* **2012**, *41*, 3878. (b) Chang, Y.-C.; Wang, S.-L. *J. Am. Chem. Soc.* **2012**, *134*, 9848. (c) Yagai, S.; Okamura, S.; Nakano, Y.; Yamauchi, M.; Kishikawa, K.; Karatsu, T.; Kitamura, A.; Ueno, A.; Kuzuhara, D.; Yamada, H.; Seki, T.; Ito, H. *Nat. Commun.* **2014**, *5*, 4013. (d) Sun, H.; Liu, S.; Lin, W.; Zhang, K. Y.; Lv, W.; Huang, X.; Huo, F.; Yang, H.; Jenkins, G.; Zhao, Q.; Huang, W. *Nat. Commun.* **2014**, *5*, 3601. (e) Liu, W.; Wang, Y.; Sun, M.; Zhang, D.; Zheng, M.; Yang, W. *Chem. Commun.* **2013**, *49*, 6042. (f) Wang, Y.; Liu, W.; Bu, L.; Li, J.; Zheng, M.; Zhang, D.; Sun, M.; Tao, Y.; Xue, S.; Yang, W. *J. Mater. Chem. C* **2013**, *1*, 856. (g) Bu, L.; Sun, M.; Zhang, D.; Liu, W.; Wang, Y.; Zheng, M.; Xue, S.; Yang, W. *J. Mater. Chem. C* **2013**, *1*, 2028.

(5) Wen, T.; Zhou, X.-P.; Zhang, D.-X.; Li, D. *Chem. - Eur. J.* **2014**, *20*, 644.

(6) (a) Long, J. R.; Yaghi, O. M. *Chem. Soc. Rev.* **2009**, *38*, 1213. (b) Zhou, H.-C.; Long, J. R.; Yaghi, O. M. *Chem. Rev.* **2012**, *112*, 673. (c) Zhou, H.-C.; Kitagawa, S. *Chem. Soc. Rev.* **2014**, *43*, 5415.

(7) (a) Lu, W.; Wei, Z.; Gu, Z.-Y.; Liu, T.-F.; Park, J.; Park, J.; Tian, J.; Zhang, M.; Zhang, Q.; Gentle Iii, T.; Bosch, M.; Zhou, H.-C. *Chem. Soc. Rev.* **2014**, *43*, 5561. (b) O'Keeffe, M.; Yaghi, O. M. *Chem. Rev.* **2012**, *112*, 675.

(8) (a) Cui, Y.; Yue, Y.; Qian, G.; Chen, B. *Chem. Rev.* **2012**, *112*, 1126. (b) Kreno, L. E.; Leong, K.; Farha, O. K.; Allendorf, M.; Van Duyne, R. P.; Hupp, J. T. *Chem. Rev.* **2012**, *112*, 1105. (c) Allendorf, M. D.; Bauer, C. A.; Bhakta, R. K.; Houk, R. J. T. *Chem. Soc. Rev.* **2009**, *38*, 1330. (d) Hu, Z.; Deibert, B. J.; Li, J. *Chem. Soc. Rev.* **2014**, *43*, 5815. (e) Shustova, N. B.; Cozzolino, A. F.; Reineke, S.; Baldo, M.; Dincă, M. *J. Am. Chem. Soc.* **2013**, *135*, 13326.

(9) (a) Shustova, N. B.; McCarthy, B. D.; Dincă, M. *J. Am. Chem. Soc.* **2011**, *133*, 20126. (b) Hu, Z.; Huang, G.; Lustig, W. P.; Wang, F.; Wang, H.; Teat, S. J.; Banerjee, D.; Zhang, D.; Li, J. *Chem. Commun.* **2015**, *51*, 3045. (c) Shustova, N. B.; Cozzolino, A. F.; Dincă, M. *J. Am. Chem. Soc.* **2012**, *134*, 19596. (d) Shustova, N. B.; Ong, T.-C.; Cozzolino, A. F.; Michaelis, V. K.; Griffin, R. G.; Dincă, M. *J. Am. Chem. Soc.* **2012**, *134*, 15061.

(10) Pearson, R. G. *J. Am. Chem. Soc.* **1963**, *85*, 3533.

(11) Wei, Z.; Gu, Z.-Y.; Arvapally, R. K.; Chen, Y.-P.; McDougald, R. N.; Ivy, J. F.; Yakovenko, A. A.; Feng, D.; Omary, M. A.; Zhou, H.-C. *J. Am. Chem. Soc.* **2014**, *136*, 8269.

(12) Hong, Y.; Lam, J. W. Y.; Tang, B. Z. *Chem. Commun.* **2009**, 4332.

(13) (a) Feng, D.; Gu, Z.-Y.; Li, J.-R.; Jiang, H.-L.; Wei, Z.; Zhou, H.-C. *Angew. Chem., Int. Ed.* **2012**, *51*, 10307. (b) Morris, W.; Volosskiy, B.; Demir, S.; Gándara, F.; McGrier, P. L.; Furukawa, H.; Cascio, D.; Stoddart, J. F.; Yaghi, O. M. *Inorg. Chem.* **2012**, *51*, 6443.

(14) (a) Jiang, H.-L.; Feng, D.; Wang, K.; Gu, Z.-Y.; Wei, Z.; Chen, Y.-P.; Zhou, H.-C. *J. Am. Chem. Soc.* **2013**, *135*, 13934. (b) Feng, D.; Chung, W.-C.; Wei, Z.; Gu, Z.-Y.; Jiang, H.-L.; Chen, Y.-P.; Darensbourg, D. J.; Zhou, H.-C. *J. Am. Chem. Soc.* **2013**, *135*, 17105. (c) Feng, D.; Gu, Z.-Y.; Chen, Y.-P.; Park, J.; Wei, Z.; Sun, Y.; Bosch, M.; Yuan, S.; Zhou, H.-C. *J. Am. Chem. Soc.* **2014**, *136*, 17714.

(15) Deria, P.; Mondloch, J. E.; Tylianakis, E.; Ghosh, P.; Bury, W.; Snurr, R. Q.; Hupp, J. T.; Farha, O. K. *J. Am. Chem. Soc.* **2013**, *135*, 16801.

(16) (a) Wan, W.; Sun, J.; Su, J.; Hovmöller, S.; Zou, X. *J. Appl. Crystallogr.* **2013**, *46*, 1863. (b) Zhang, D.; Oleynikov, P.; Hovmöller, S.; Zou, X. *Z. Kristallogr.* **2010**, *225*, 94.

(17) Zhou, H.-L.; Zhang, Y.-B.; Zhang, J.-P.; Chen, X.-M. *Nat. Commun.* **2015**, *6*, 6917.

DOI: 10.1021/jacs.5b04695
J. Am. Chem. Soc. 2015, 137, 10064−10067